

Virtual ROPS and FOPS Testing on Agricultural Tractors According to OECD Standard Code 4 and 10

D. Hailoua Blanco*, C. Martin*, A. Ortalda*

*EnginSoft S.p.A

Abstract

The Roll Over Protection Structure (ROPS) and Falling Object Protective Structure (FOPS) are key safety features in agricultural and forestry tractors in order to avoid or limit risks to the driver in case of roll over or falling objects during normal use.

The Organization for Economic Co-operation and Development (OECD) in an effort to improve operator's safety in Agricultural and Forestry Tractors has set up harmonized testing procedures for ROPS and FOPS systems. The current OECD Codes for tractors relate to several features of performance. In particular, Code 4 and 10 are related to the strength of protective structure in case of roll over and falling objects, respectively [1-2].

On the one hand, Code 4 foresees a sequence of loadings that the protection system has to withstand until the prescribed energy or force is satisfied. The magnitude of the required energy and forces depend upon the reference mass of the tractor. In addition to successfully resist the loading sequence, the ROPS has to guarantee a clearance zone during any part of the tests around the seat index point (SIP), where the operator is placed. By fulfilling all these conditions, the structure is classed as a roll-over protective structure in accordance with the OECD Code 4.

On the other hand, Code 10 implies a series of object drop tests from a height to develop a specific energy. Likewise, the clearance zone shall not be entered by any part of the protective assembly or the impacting object itself to pass the test.

In light of the complex testing scenarios, numerical simulations with LS-DYNA[®] were carried out to virtually assess the performance of a ROPS and FOPS system designed by the Italian tractor manufacturer. As a matter of fact, ROPS and FOPS simulations turned out to be very useful to understand the behavior of the protection system subjected to complex loading and get valuable insights into performance. The main goal of the simulations was to virtually test the tractor according to the Code 4 and 10 prior to official test approval and, if necessary, introduce the necessary structural changes in order to successfully pass the ROPS and FOPS tests.

Keywords: ROPS, FOPS, Tractors

Introduction

The main goal of the Roll Over Protection Structure (ROPS) and Falling Object Protective Structure (FOPS) is to provide protection to the operator in case of roll-over accident and falling objects, respectively. Such passive safety features are commonly found in nowadays agricultural and forestry tractors and are conceived to protect the operator from a serious injury or even death in case of an unexpected accident. Agricultural accidents may be caused by improper maneuvers, hill falls, road accidents and in such cases the protective systems must be able to absorb the impact energy without endangering the driver.

In an effort to improve the operator's safety in agricultural and forestry tractors, the Organization for Economic Co-operation and Development (OECD) has established worldwide some standards to harmonize the protective equipment testing and therefore facilitate international

trading. Since its foundation in 1961, many countries have joined and agreed on a wide range of standards other than agricultural.

In the current work, the OECD Code 4 and 10 have been numerically studied which are related to tractor ROPS and FOPS performance, respectively. The Code 4 sets up requirements in terms of energy or force for the longitudinal, lateral and vertical directions of the cabin structure, while the Code 10 implies a series of drop tests to test the upper head protective assembly against falling objects. Besides structural resistance, both codes define a clearance zone where the driver should be seated, which has not to be entered by any part of the structure or impacting object at any time.

LS-DYNA® has been demonstrated to be a suitable tool to investigate the ROPS and FOPS performance in the early stage of the design phase due to several reasons:

- Robust contact algorithms.
- MPP scalability (Massively Parallel Processing).
- Available material models.
- Full-restart feature.

As stated above, the ROPS testing foresees a sequence of longitudinal, lateral and vertical loads on the cabin. By using the LS-DYNA® full-restart feature [3], the full history of the ROPS structure could be taken into account up to the restart point without having to re-run the complete sequence. By doing so, the new pushers could be added and positioned in the model to keep on with the virtual testing. This feature extremely saved CPU time and speeded up the engineering process.

Numerical simulations with LS-DYNA® virtually assessed the performance of the ROPS and FOPS structures designed by Argo Tractors S.p.A according to OECD Code 4 and 10. Therefore, the confidence in successful ROPS and FOPS approval was raised and confirmed by experimental testing.

The current paper will show the main aspects regarding the ROPS and FOPS modeling with LS-DYNA. The correlation between experimental and numerical results will be shown for the ROPS study as there was not available experimental data for the FOPS test while writing the current paper. In the meantime, the tractor has been approved for both ROPS and FOPS and it is currently available in the market under the Landini brand.

Brief tractor description

The protective structure (ROPS) is mainly made of a reinforced tubular welded steel frame which is joined to the tractor chassis by means of the platform (See Fig.1). The platform is the lower part of the protective structure which is fixed to the tractor by four supports. Silent blocks are mounted on the front and rear supports in order to provide cushion and therefore comfort to the driver.

The protective structure (FOPS) is an assembly mainly made of plastic materials which is designed to provide overhead protection to the driver.

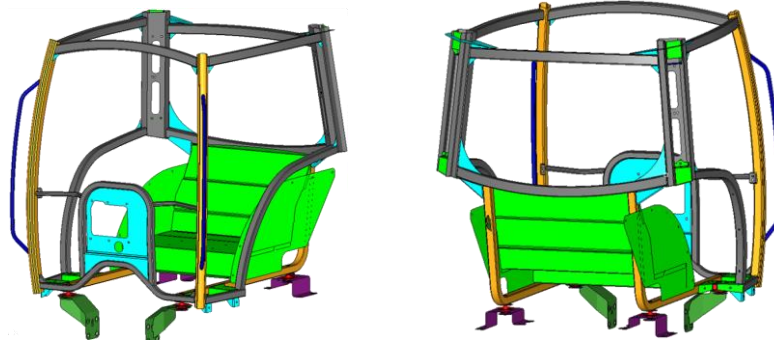


Fig.1 CAD model of the tractor protective structure ROPS.



Fig.2 CAD model of the tractor showing the protective structure FOPS.

Test description

Code 4 - ROPS

According to OECD Code 4, the ROPS tests shall be conducted in the following sequence:

1. Longitudinal loading
2. Rear crushing
3. Side loading
4. Front crushing

For further details about the pushers (geometry, location), clearance zone etc. the reader is referred to the Code 4 reference [1].

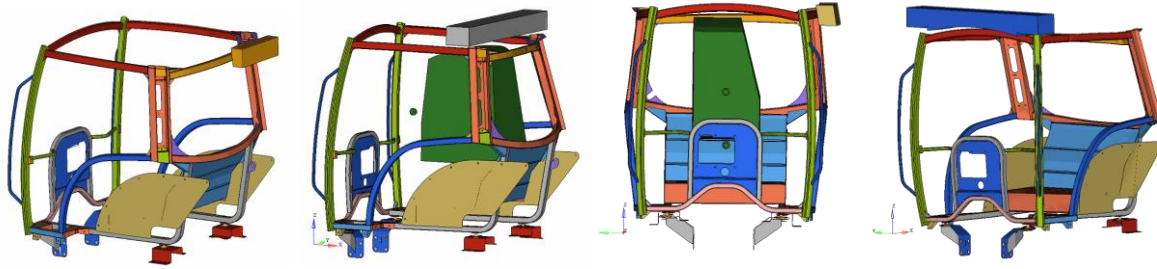


Fig.3 ROPS sequence – longitudinal, rear, side and front loads, respectively.

Longitudinal and side loadings have to fulfill the requirement of energy absorption, while rear and front crushing have to sustain the prescribed loads. In any of those cases, the clearance zone (central green box in Fig.3 has not to be entered by any part of the structure to pass the test. The magnitude of the required energy as well as crushing force depends upon the reference mass of the tractor, in this case, 4400 kg. The rate of load application shall be such that it can be considered as static. This was numerically done in the simulation by carrying out a quasi-static analysis. That is, using the explicit dynamics solver, the pusher's speed was selected such that the kinetic energy of the system remained below the total internal energy a couple of orders of magnitude. Hence, minimizing the inertial effects.

It is pointed out that the required energy is the product of the pusher's displacement by the necessary force to deform cabin. Each load step implies a loading and unloading phase. The key aspect about ROPS testing is that all loading steps are linked, that is, the deformation of cabin at the first loading step will influence the following ones and so forth. Therefore, only after the unloading phase, the location of the pusher for the next load step can be determined.

In other words, the position of all the pushers cannot be known in advance since it depends on the deformation history of the cabin. For instance, the user cannot predict the necessary displacement to fulfill the energy requirement in the first load step, therefore, such displacement has to be tracked down and once achieved, re-run the simulation with the unloading phase (simply moving the pusher backwards).

This can be time consuming since the first loading step will require 2 simulations, the second one will require 1 simulation (rear crushing implies only a requirement in terms of force, not energy), the third will require 2 simulations (loading up to the prescribed energy and unload) and last one will require 1 simulation. In total, 6 simulations are necessary. The time consuming task is that each of the subsequent simulations need to re-run the previous steps. Therefore, the possibility to output restart files by LS-DYNA is of great value since can save lots of CPU time. Specifically, the full-restart allows to include new parts such as the pushers. The only keyword that the user needs to set up is the *STRESS_INITIALIZATION to initialize the old parts in the restart phase.

In the following Fig.4, the loading sequence is summarized along with the energy and force requirements:

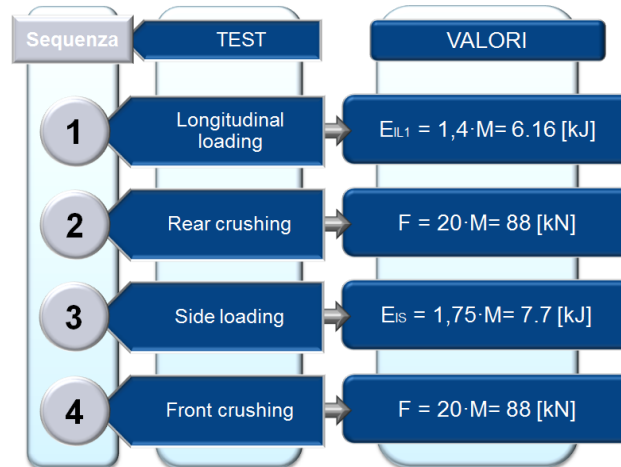


Fig.4 Loading sequence for Code 4. M (reference mass) = 4400 kg

Code 10 – FOPS

The OECD Code 10 states that the drop test object shall be a spherical object dropped from a height sufficient to develop 1365 J. The drop object shall be made of solid steel or ductile iron sphere with a typical mass of 45 kg and a diameter between 200 and 250 mm (220 mm employed in the current study). Three different impacts in sequence were chosen for the current investigation as shown in the following Fig.5.

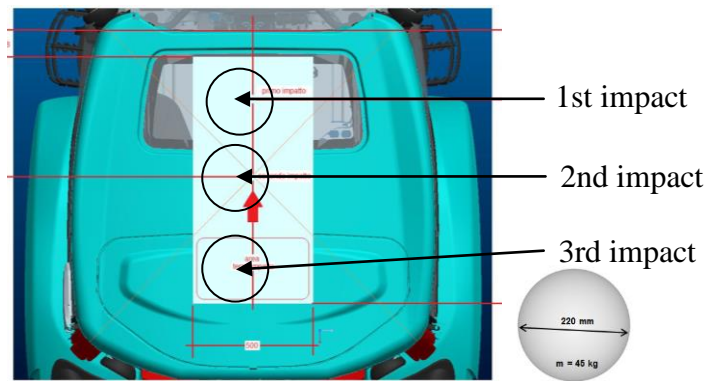


Fig.5 FOPS impact sequence

FE Modeling

Two different FE models were created.

A first model was built up for the ROPS testing and a second one including the overhead assembly for the FOPS testing.

ROPS structure (cabin)

The cabin CAD geometry was accurately meshed with 2D shell elements since most of the components were tubular steel frames and thin metal sheets.

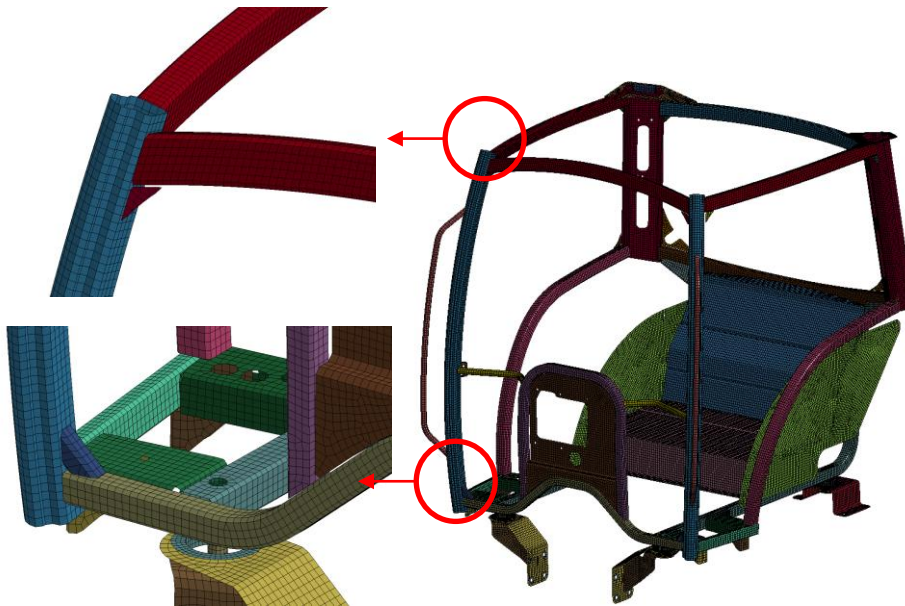


Fig.6 Meshed main protective structure for ROPS and FOPS test

Average mesh size of 10 mm, corresponded to a good trade-off between accuracy and computational time. In fact, the average mesh size was reduced from 15 mm down to 5 mm to study the mesh influence on the obtained results. It was recognized that the 10 mm mesh size provided meaningful convergence.

The total number of elements corresponded to 80207 shell elements. Fully integrated formulation (ELFORM=16) was employed for the study [4].

Sheet metal pieces were connected (welded) using the *CONSTRAINED_NODAL_RIGID_BODY option in LS-DYNA. Therefore, welds were modeled as a non-breakable connections between parts. In fact, this approach was very useful at the early design stage to identify potential critical areas. In such cases, more detailed methods using continuum elements were used to evaluate weld failure. Nodal rigid body spiders were also used to model bolted connections.

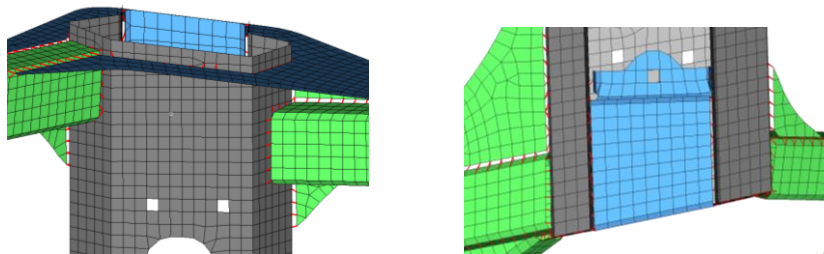


Fig.7 Mesh details showing an example of the *nodal_rigid_body welds (red connections)

*MAT_24 (elastoplastic) with experimental tensile true stress-strain curves was used to characterize the steels in the cabin. In particular, mainly three types of steel were employed: S-235, S-275 and S-355 (UNI EN 10025).

The clearance zone was defined according to the seat index point (SIP) and the reference plane for seat. To keep track of the clearance zone during the simulation, its external skin was modeled (mesh) with 2D thin shell elements and assigned a rigid material. Such volume was connected to the horizontal platform by means of beam elements using *CONSTRAINED_INTERPOLATION.



Fig.8 Mesh detail showing the anchoring points of the clearance zone

The easy to use *CONTACT_AUTOMATIC_SINGLE_SURFACE was used for all the cabin components. This contact takes into account potential self-contacts as well as contact between components (including shell thickness). From the user point of view, the definition of such contact only requires a set of *PARTs in the model so it can be immediately defined without needing to individually search for potential interacting parts.

The tractor was fixed to the ground by means of four supports (bolted connections) using the *MAT_20 (rigid) constraint parameters (CON1=CON7=7) on the washer's area.

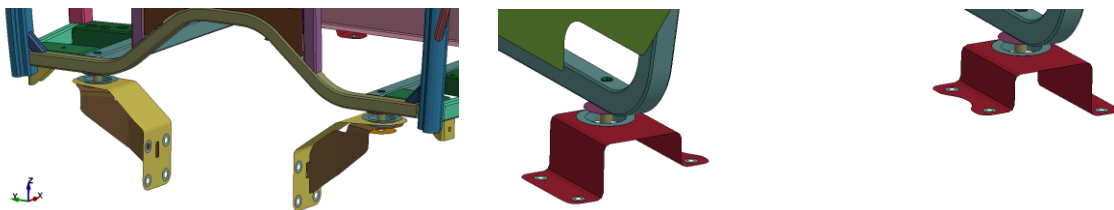


Fig.9 Front and rear supports of the tractor

Silent Blocks

The cabin is suspended by means of the rubber silent blocks, which are components for absorbing and dampening vibrations in order to increase the driving comfort. They are located two at the front supports and two at the rear ones.

The behaviour of the silent block was modeled with beam elements (ELFORM=6). The radial and longitudinal stiffness were set up according to experimental results. To do that, *MAT_GENERAL_NONLINEAR_6DOF_DISCRETE_BEAM was employed. Such material model allows for the definition of an arbitrary translational force curve along the local axis of the

beams. Hence, it is very useful to define different axial as well as radial behaviour, including bottoming out, where the rubber material cannot further absorb energy and becomes stiff. This effect can be easily taken into account by means of a steep increase in the force vs displacement behaviour.

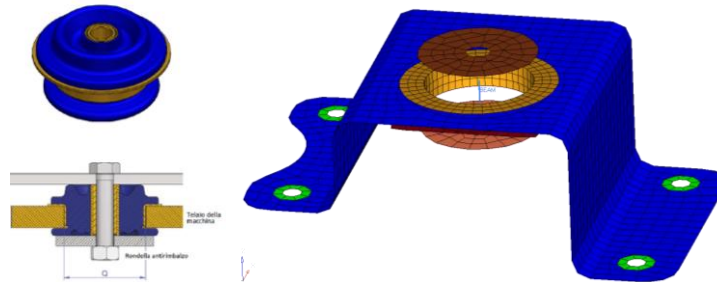


Fig. 10 Example of rear cabin support with the silent block modeling

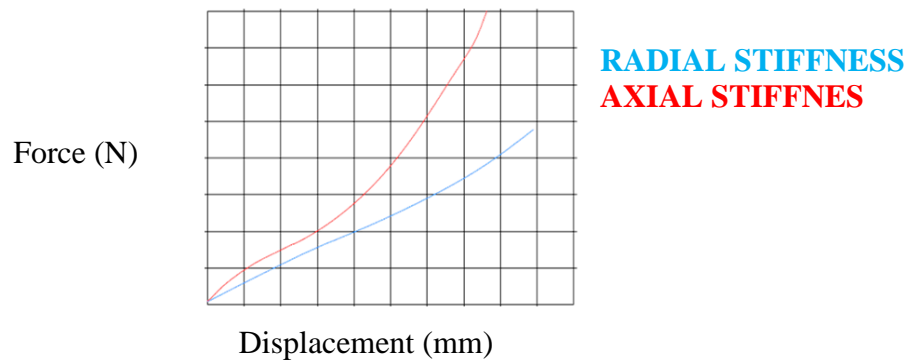


Fig. 11 Axial and radial stiffness for the silent blocks

Pushers

In a ROPS test, the pushers are the components that transmit forces to the cabin in order to achieve certain amount of energy (force vs displacement) or simply, specific crushing force value.

The load to the ROPS structure needs to be uniformly applied by means of a stiff beam (normal to the direction of the load). Such beams are bound in order to prevent lateral displacement. Experimentally, as the load is applied (typically by means of a hydraulic system), force and displacements are recorded. Numerically, the force was the result of a prescribed motion to the pushers.

Specifically, the pushers were modeled as a rigid components and a specific `*CONTACT_AUTOMATIC_SURFACE_TO_SURFACE` was assigned between such component and the rest of the cabin. The universal type of joint between the hydraulic piston and the stiff beam was directly modeled using the constraint rigid body motion (CON1 and CON 2) included in the `*MAT_RIGID` (`*MAT_20` card).



Fig.12 Hydraulic piston and respective rotation due to the universal joint

As a matter of fact, CON1 and CON2 parameters allow the user to specify the translational and rotational constraints with respect to the calculated center of mass of the rigid body. Therefore, the real behavior of the hydraulic cylinder can be easily approximated using the appropriate translation and rotational constraints. Alternatively, a *CONSTRAINT_JOINT_UNIVERSAL located at the center of rotation could be added.

FOPS structure (roof)

The FOPS structure is an overhead assembly which is conceived to transfer the impact loadings due to potential falling objects to the cabin structure.

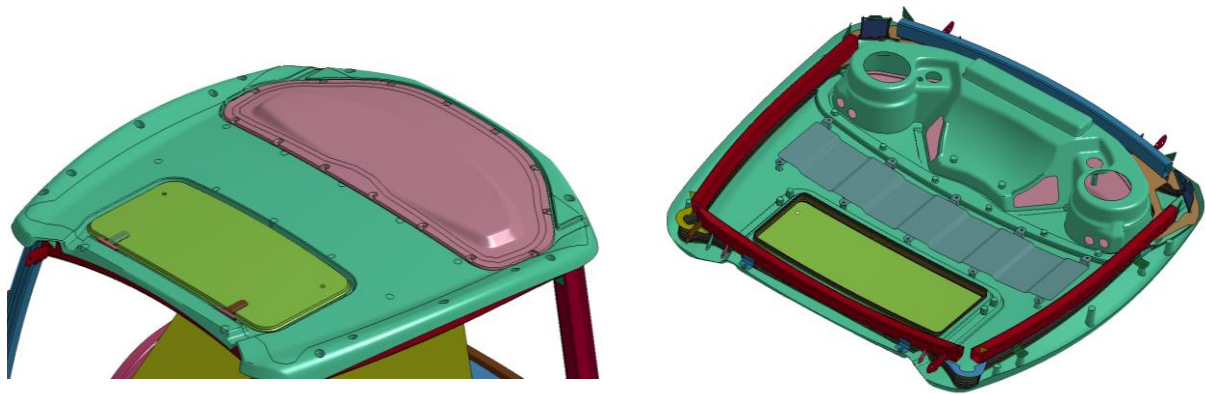


Fig.13 Overview of FOPS protective structure

The model consisted of 338K shell elements varying from 2.5 to 6 mm depending upon the component. Full integrated formulation (ELFORM=16) was used. In this case, the mesh size was reduced to 5 mm to better capture plastic strain gradients on the components. The bolted connections between components were modeled with rigid body spiders (*CONSTRAINED_NODAL_RIGID_BODY).

Most of the materials encompassing the overhead assembly are plastics with the exception of the central reinforcement plate which is made of steel S-235. The plastic material was characterized by *MAT_24 (elastoplastic) where the tensile stress-strain behavior was added as an input curve. No failure was implemented in the model, so plastic strains along with engineering judgement were used to identify critical areas.

Results and Discussion

Simulations were carried out using LS-DYNA® MPP R8.0.0d @ 16 CPUs - Intel Xeon® E5-2680 v2 @ 2.8 GHz. Since ROPS tests were needed to be quasistatic, this implied longer simulation times than standard explicit. In the current study, about 3 seconds were simulated. The total amount of time required for all the steps was about 40 hours. Hence, the importance of the LS-DYNA® full restart feature.

The FOPS test was a standard drop test. The important thing was to wait between impacts to stabilize the cabin from silent block vibrations. As a result, between 150 and 200ms were needed in between impacts. In this case 500 ms were simulated and the required time was about 30 hours.

ROPS

In the following paragraphs (0 - 0) a comparison will be shown between the numerical and experimental approval results. It is pointed out that such experimental ROPS phase were only done after the numerical results met the code 04 requirements.

As a matter of fact, numerical forces as a result of the pusher's action were recorded with time and compared to the experimental results for the longitudinal and side loading. The prescribed energy was simply obtained by integrating the force vs displacement curve. Regarding the crushing tests, the compression force was applied at the corresponding location but with no displacement recorded. The likelihood of failure was evaluated by looking at the accumulated equivalent plastic strains during the test.

Longitudinal loading

As described in the Fig.4, the main goal of this test was to achieve 6.16 kJ of absorbed energy by applying a longitudinal load and most importantly, guarantee the clearance zone.

The overall behavior of the ROPS structure was in accordance to experimental results as depicted in the Fig.14. In addition to this, the force vs displacement curves were in agreement as shown in Fig.15.

The stiffness of the cabin is well predicted in the first part of the test (see Fig.15) where the main tubular structure is in elastic regime. Nonetheless, once the stresses on the tubular components start exceeding the yield strength, the slope begins to decrease significantly in comparison to the experimental test. This difference may be mainly attributed to the material model as well as the cold forming history of the components which has not been taken into account. It is pointed out that no reverse engineering was done to tune the material model since the characterization was done prior to testing. Hence, further improvement of the results can be expected by numerical tuning of the steel materials but this was not the objective of the current study.



Fig.14 Numerical ROPS prediction vs real test for longitudinal loading @ 6.16 kJ

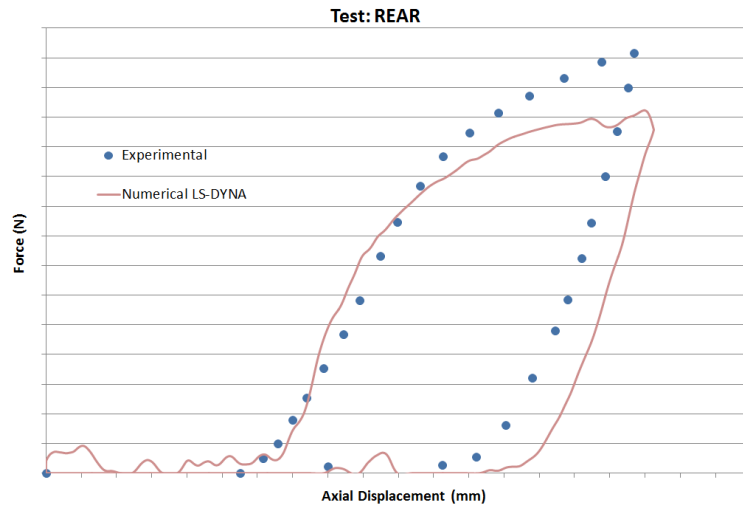


Fig.15 Experimental vs numerical force for rear longitudinal loading (ROPS)



Fig.16 Longitudinal loading. Grey: elastic region areas. Colored: main plastic strain areas.

None of the plastic deformations found in the ROPS were considered to be critical (Fig.16). Concerning the clearance zone, none of the structural components entered into the volume. The critical state, which corresponds to the maximum longitudinal displacement at 6.16 kJ did not penetrate the clearance zone. Such state can be observed in the following Fig.17.

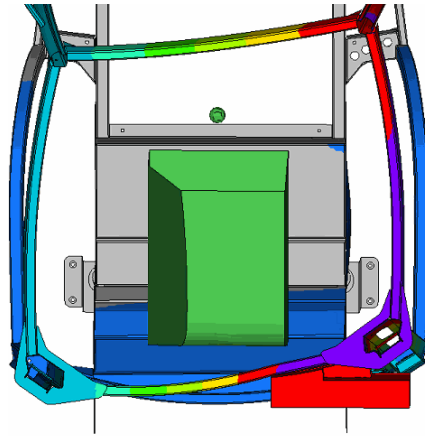


Fig.17 Top view of ROPS structure with clearance zone (green box) @ 6.16 kJ



Fig.18 Numerical deformation vs experimental test after the longitudinal test

Rear crushing

The aim of this test was to apply a compressive load of 88 kN on the rear side of the ROPS structure.



Fig.19 Numerical vs experimental rear crushing test

The ROPS structure was well designed as it could withstand the load 88 kN without compromising the clearance zone (see Fig.20). On the other side, the new plastic strains introduced on the structure were limited and therefore not critical (see Fig.21).

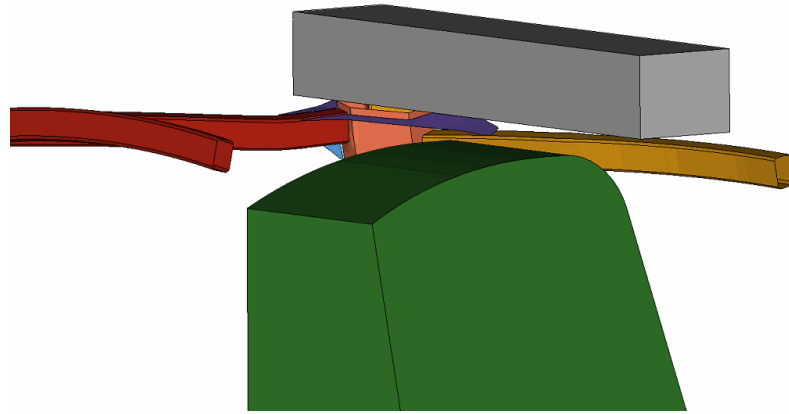


Fig.20 Relative position of the clearance zone respect to ROPS structure for rear crushing

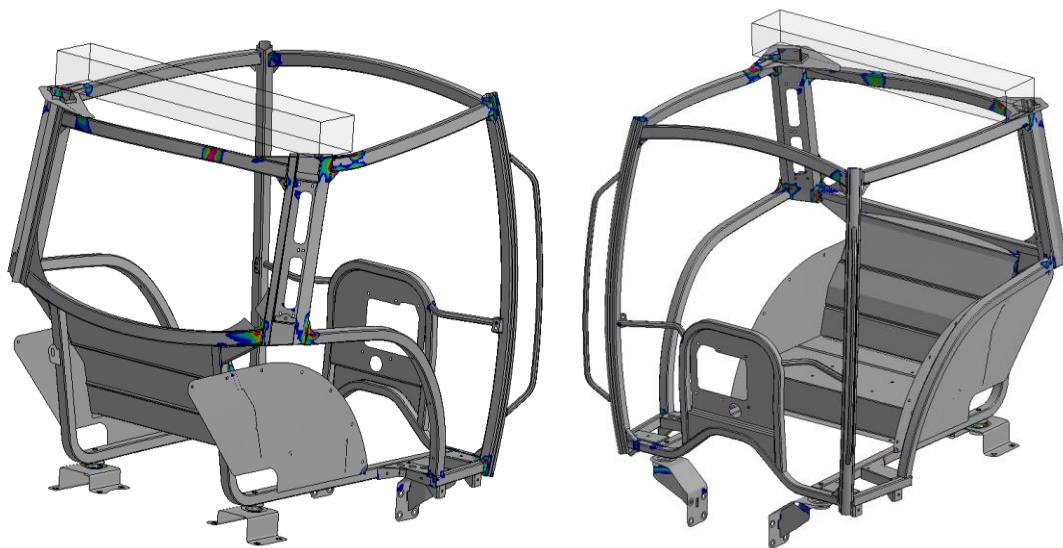


Fig.21 Rear crushing. Grey: elastic region areas. Colored: main plastic strain areas.

Side loading

According to the standards, after the rear test, it was sequentially applied the side loading to achieve 7.7 kJ of energy absorbed.

It is noticed that once a test is successfully passed, the pushers are positioned and the test is started. To take into account the history of the ROPS structure (plastic strains, stresses, and updated geometry) and speed up the engineering process, the full restart feature was sequentially used as well. Hence, there was no need to re-run the previous load steps to keep on with the ROPS study.

The ROPS structure showed good agreement in terms of deformations as well as loading response (force vs displacement). In this case, the numerical behavior of the ROPS structure seemed to be stiffer compared to the experimental test (Fig.23). As a matter of fact, the

numerical curve is mainly above the experimental one, meaning that the energy time calculated by integrating the curve will be higher as well. Despite of this fact, the results were satisfactory.

New plastic strains were not critical based on engineering judgment and the clearance zone was preserved.



Fig.22 Numerical vs experimental side loading test

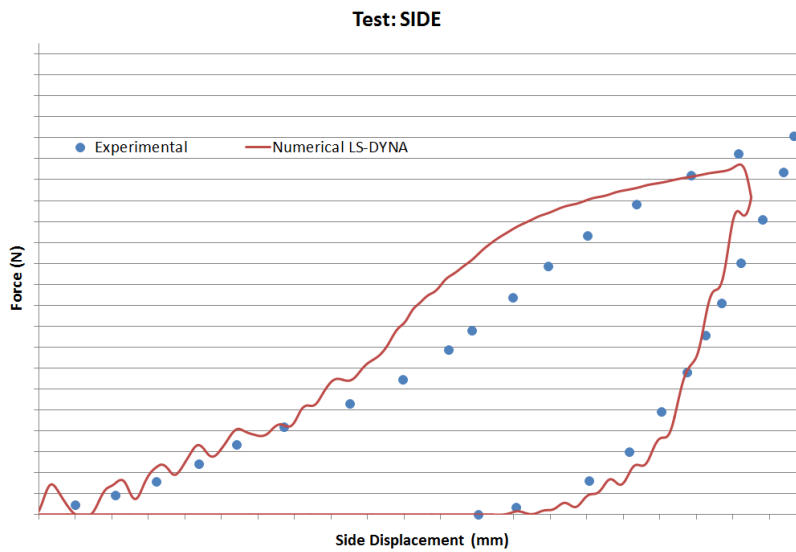


Fig.23 Experimental vs numerical force for side loading (ROPS)

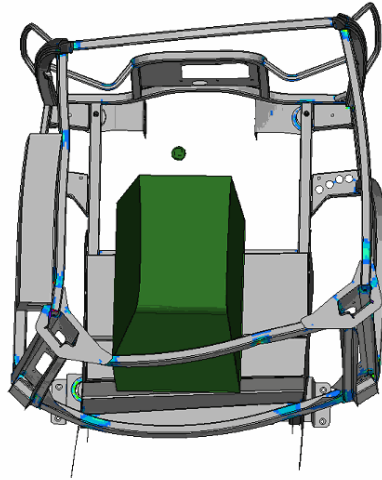


Fig.24 Relative position of the clearance zone respect to ROPS structure for rear crushing

Front crushing

The final test of the ROPS sequence is the front crushing. As for rear crushing, the force applied to the front side of the cabin was 88 kN. No particular weak points were found in the structure and the clearance zone therefore guaranteed.

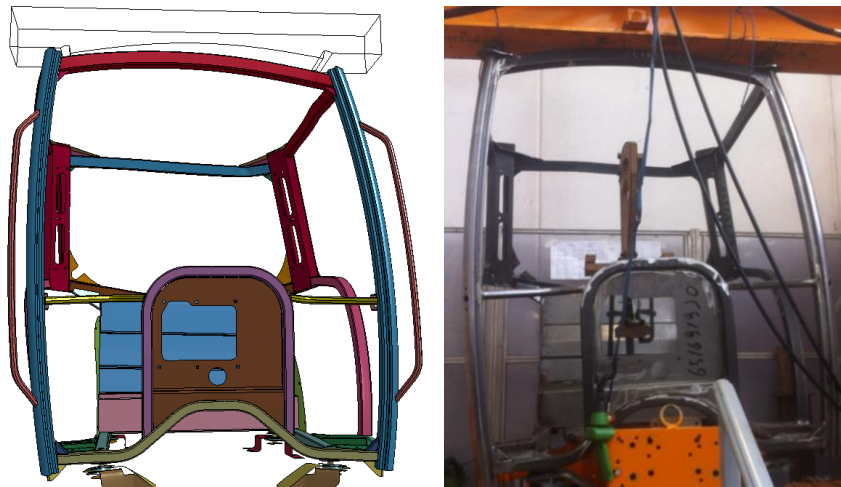


Fig.25 Numerical vs experimental front crushing test

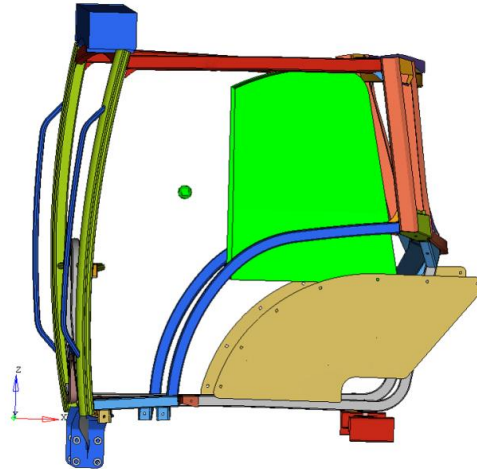


Fig.26 Relative position of the clearance zone respect to ROPS structure for front crushing



Fig.27 Front crushing. Grey: elastic region areas. Colored: main plastic strain areas.

After such test, the ROPS structure numerically met the Code 4 requirements and therefore was ready for the approval test. In agreement with numerical findings, the experimental ROPS results did not show particular failure areas.

FOPS

In this phase, 3 sequential sphere impacts on the FOPS structure was numerically investigated. On the one hand, it was checked the maximum deflection of the overhead protection did not interfere with the clearance zone. On the other hand, maximum plastic strains were analyzed to assess the likelihood of failure since the material failure was not implemented in the model.

First Impact

For this impact, high plastic strain values were found at the pinned connection of the top hatch (Fig.30). At first glance such plastic strains may not seem critical but possible differences in mechanical properties (scatter) due to manufacturing reasons, may cause local failure. Simulations showed that the clearance zone is guaranteed provided that no failure occurs at the opening / closure mechanism. For such reason, although not shown in the current study, the mechanism was reinforced prior to approval testing.

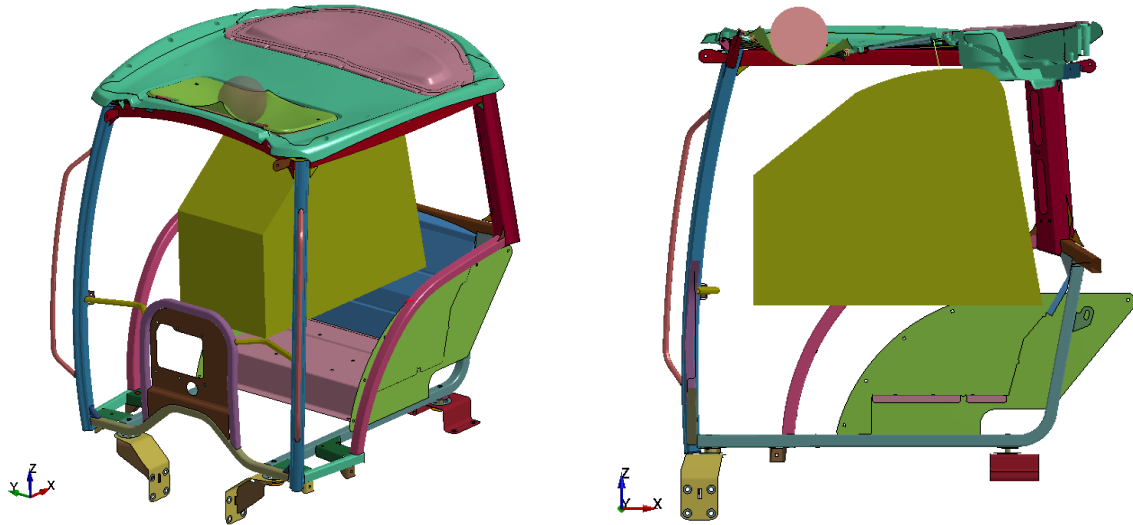


Fig.28 FOPS first impact

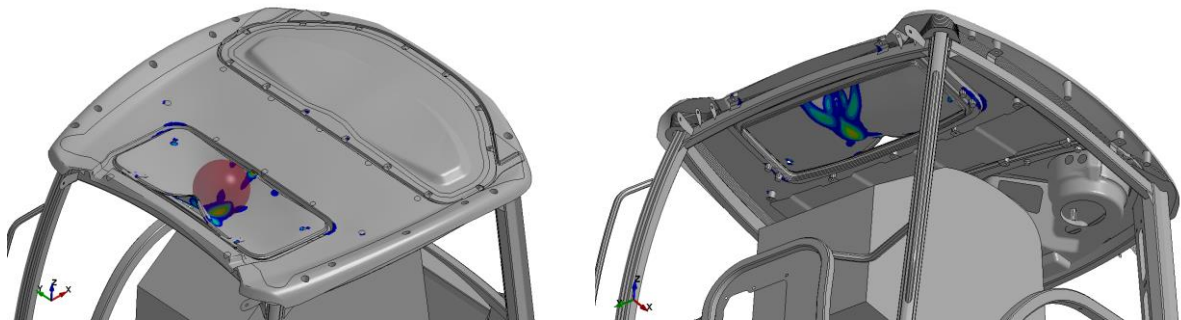


Fig.29 FOPS first impact. Grey: elastic region areas. Colored: main plastic strain areas.

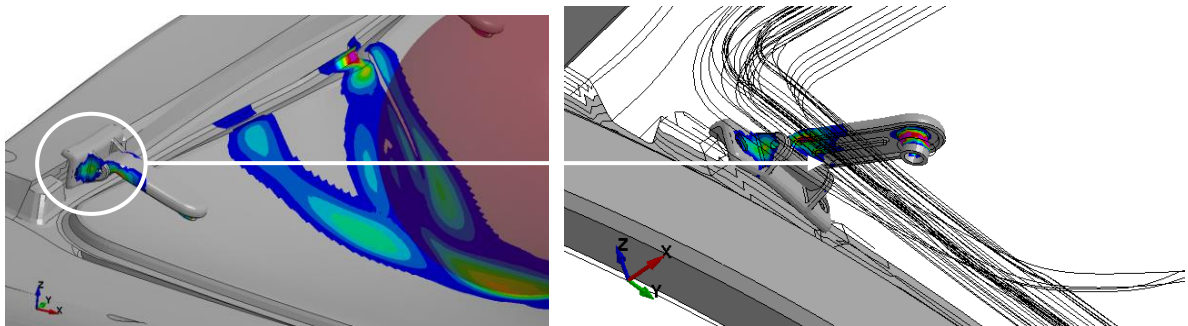


Fig.30 Main plastic strains on FOPS protective structure for the first impact

Second Impact

The second impact guaranteed the clearance zone. Limited plastic strains were located at brackets of the metal sheet reinforcement. Such reinforcement was important to contain the maximum deflection caused by the steel ball. No critical areas were found.

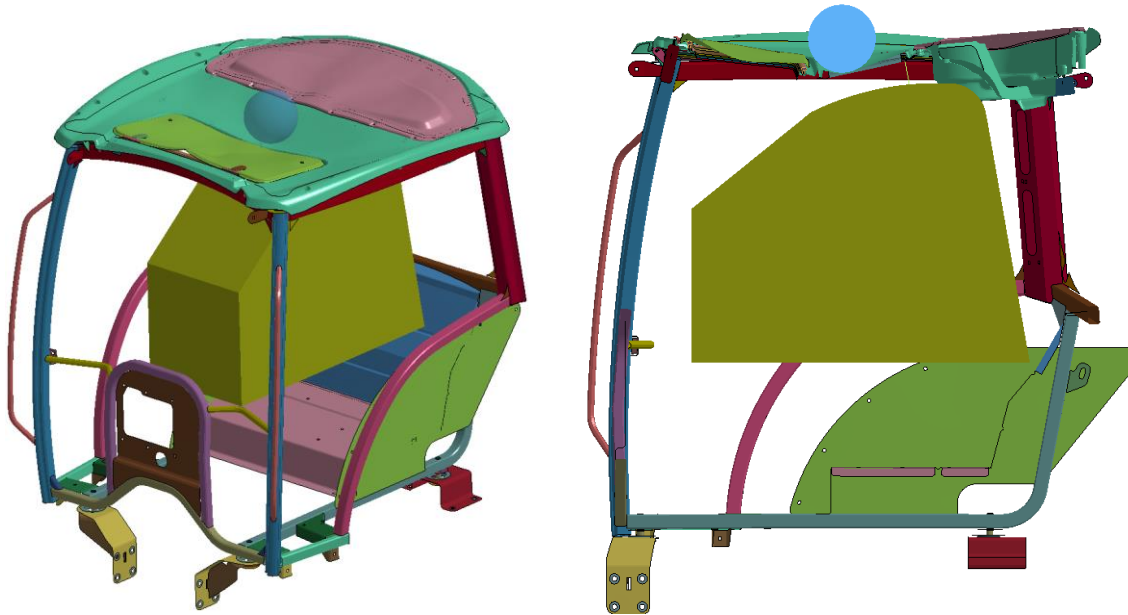


Fig.31 FOPS second impact

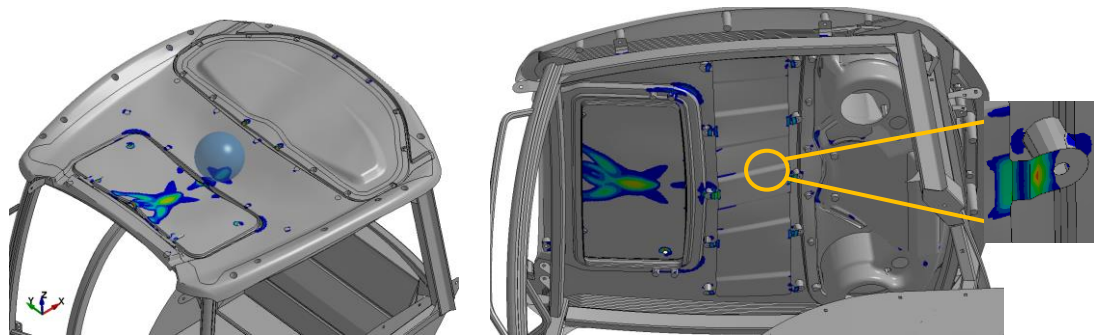


Fig.32 FOPS second impact. Grey: elastic region areas. Colored: main plastic strain areas.

Third impact

Some critical areas in terms of plastic strain were found at top lid bolted connections meaning that local failure may occur (see Fig.34). Moreover, despite of the fact that the clearance zone was guaranteed, the distance between the overhead assembly and the clearance zone (at the maximum deflection point) was not enough to face with confidence the experimental test. Hence, further improvements not shown in the current study were introduced to conservatively handle possible misalignments with the real test. After analyzing the first and third impact and implementing the modifications, the experimental FOPS approval test was done and passed.



Fig.33 FOPS third impact

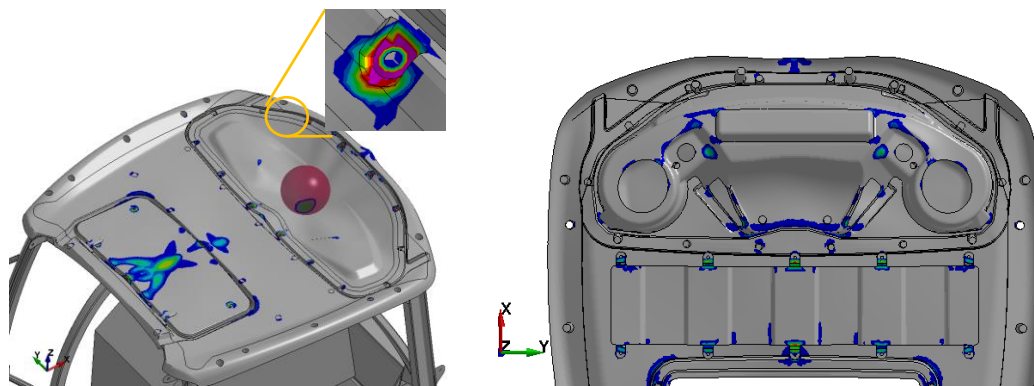


Fig.34 FOPS third impact. Grey: elastic region areas. Colored: main plastic strain areas

Summary of tests

ROPS

All ROPS steps were successfully passed.

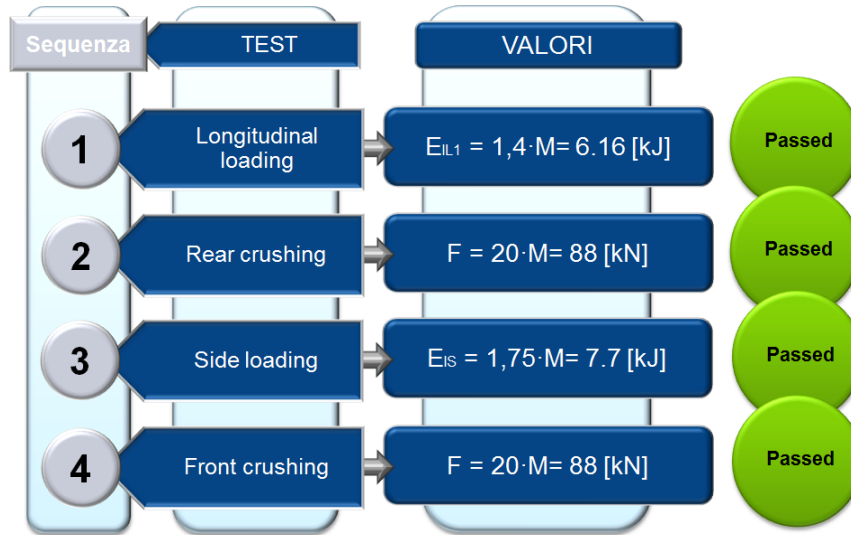


Fig.35 Summary of the ROPS tests sequence

FOPS

All FOPS steps were successfully passed. However, some critical areas were found and the final overhead protection system was reinforced. The final version of the overhead assembly improved the results showed in the current study.

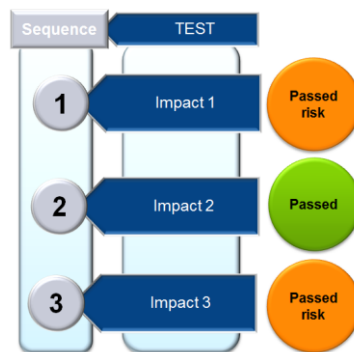


Fig.36 Summary of the FOPS sequence

Conclusion

LS-DYNA was proved to be a very useful tool to predict the ROPS and FOPS behavior in the early stage design phase. In fact, ROPS experimental testing confirmed numerical findings in terms of loading response and stressed areas. Likewise, FOPS study give valuable insights into overhead performance and as result critical areas were reinforced.

It is important to notice that the user took advantage of the full-restart feature along MPP scalability (Massively Parallel Processing) to save CPU time and speed up the engineering

process. In addition to this, the models were very robust (despite of large deformations, nonlinear material behavior and contacts) giving rise to consistent results.

The added value of simulation was demonstrated that the post processing results were used to give a cutting edge advantage over traditional design methods in order to assess performance. As a matter of fact, critical points were identified and modifications were done quickly (in FE ambient, without needing to build the CAD model) to improve results. By doing so, the behavior of the ROPS and FOPS structure under complex loading scenarios was understood and therefore the experimental approval tests were faced with confidence.

In the end, the tractor was approved for ROPS and FOPS standards [1-2] and now can be found in the market.

References

- [1] OECD Standard Code for the official testing or protective structure on agricultural and forestry tractors. Code 04. February 2016.
- [2] OECD Standard Code for the official testing or protective structure on agricultural and forestry tractors. Code 10. February 2016.
- [3] LS-DYNA® Theory Manual, March 2006, John O. Hallquist, LSTC.
- [4] LS-DYNA® User's Keyword Manual R8, 2015, LSTC.